

# Optimal Frequency Configuration for Dual One-Way Ranging Systems

Jeongrae Kim\*

*Hankuk Aviation University, Goyang-City 412-791, Republic of Korea*

and

Byron D. Tapley†

*University of Texas at Austin, Austin, Texas 78759*

**Dual one-way ranging systems measure intersatellite distance with very high precision by combining the one-way range measurements from two satellites. This high precision is obtained by minimizing the oscillator noise effect, which is the main error source for microwave ranging systems. A key requirement for the dual one-way ranging system is the synchronization of the two one-way range measurement times, and this requirement makes it necessary to compute a high-accuracy clock solution. An optimal frequency configuration is proposed to mitigate the time-synchronization requirement. Numerical simulations demonstrate that the optimal frequency configuration becomes very effective when the clock offsets are not well known.**

## Introduction

IN recent years, the need to measure intersatellite distance with high accuracy has emerged with increasing interest in satellite formation flying. One of the ways of measuring the intersatellite distance is the use of a microwave ranging system to count the number of carrier-phase cycles. The accuracy of this type of system is mainly limited by the instability of the oscillator that drives the carrier-phase signals. A dual one-way ranging (DOWR) system minimizes the oscillator noise effect by combining the one-way range measurements from two microwave ranging systems.<sup>1–3</sup> With identical transmission and reception subsystems, each satellite transmits a carrier-phase signal to the other satellite. The received signal at each satellite is recorded and later transmitted to a control segment, for example, a ground station. The frequency fluctuations due to oscillator instability have nearly equal and opposite effects on each satellite's measurement, and summation of these two phases cancels most of the oscillator noise. The combined phase measurement is converted to the biased range between the two satellites with very high precision.

The DOWR system was first implemented on the Gravity Recovery and Climate Experiment (GRACE) mission, which consists of two coorbiting low-Earth-orbit satellites separated in orbit by about 220 km (Refs. 4 and 5). It is a dedicated spaceborne mission designed to map the gravity field with high accuracy, and its DOWR system measures the intersatellite distance with micrometer-level accuracy. Two GRACE satellites were successfully launched in March 2002 and started their five-year mission.

The GRACE DOWR system is called a K-band ranging (KBR) system because it uses K (24-GHz) and Ka (32-GHz) band frequencies. Although it might not be possible to evaluate the KBR flight performance directly, certain analysis shows that the accuracy is close to 10- $\mu$ m level,<sup>6,7</sup> as predicted level from ground tests and numerical simulations.<sup>8</sup> The new gravity field from the GRACE mission has improved our knowledge of Earth's gravity by an or-

der of magnitude. This improvement also serves to demonstrate the performance of the KBR because it is the main instrument of the GRACE satellites.

A key requirement for the DOWR is the measurement time synchronization; the measurement epoch of two satellites' phases should be very close to maximize the noise cancellation. Because the phase noise cancellation is based on the characteristic that the same noise exists in both measurements, time mismatching of the two measurements degrades the noise cancellation performance. In the case of the GRACE, the time-tag synchronization requirement is less than 150 ps. The GRACE onboard global positioning system (GPS) receiver provides this time-tag information, but this level of accuracy is hard to achieve in space in real time. Therefore, ground postprocessing with external data, for example, International GPS Service data, is necessary to achieve this level of accuracy.<sup>6,7</sup> This synchronization requirement limits the DOWR applications to post-processing missions.

This research introduces a new approach to mitigate the time-synchronization requirement. With optimally selected carrier-phase frequencies, it becomes possible to remove nearly all of the time-tag error effect and the necessity of time synchronization.

## DOWR Measurements

Carrier-phase measurement received at the two satellites at a specified nominal time  $t$  can be modeled as follows.<sup>6,8–10</sup>

Satellite A:

$$\varphi_A^B(t + \Delta t_A) = \varphi_A(t + \Delta t_A) - \varphi^B(t + \Delta t_A) = R(t)/\lambda_{A/B} + E_A \quad (1)$$

Satellite B:

$$\varphi_B^A(t + \Delta t_B) = \varphi_B(t + \Delta t_B) - \varphi^A(t + \Delta t_B) = R(t)/\lambda_{B/A} + E_B \quad (2)$$

where  $\varphi_A^B$  and  $\varphi_B^A$  represent the phases measurements at satellite A and B, respectively, which are the difference between received ( $\varphi^A$  and  $\varphi^B$ ) and reference phases ( $\varphi_A$  and  $\varphi_B$ ). The transmitted phase is identical with the reference phase. Satellite A's actual measurement time is different from the nominal epoch  $t$  by as much as  $\Delta t_A$ . The measurement time error for satellite B is  $\Delta t_B$ . Each phase measurement consists of the intersatellite range  $R(t)$ , phase wavelength  $\lambda_{A/B}$  or  $\lambda_{B/A}$ , and an error term  $E_A$  or  $E_B$ .

Dual one-way phase is defined as the summation of the two one-way phases of Eqs. (1) and (2). With this summation, most of the phase errors are canceled out except short-period variation having duration less than the time-of-flight of the microwave signal. In the case of the GRACE, the signal time-of-flight time is about 1 ms. Dual one-way range is obtained by multiplying the dual one-way

Received 14 April 2004; revision received 3 August 2004; accepted for publication 24 August 2004. Copyright © 2004 by the American Institute of Aeronautics and Astronautics, Inc. All rights reserved. Copies of this paper may be made for personal or internal use, on condition that the copier pay the \$10.00 per-copy fee to the Copyright Clearance Center, Inc., 222 Rosewood Drive, Danvers, MA 01923; include the code 0022-4650/05 \$10.00 in correspondence with the CCC.

\*Assistant Professor, School of Aerospace and Mechanical Engineering; jrkim@hau.ac.kr. Senior Member AIAA.

†Clare Cockrell Williams Chair and Director, Center for Space Research; tapley@csr.utexas.edu. Fellow AIAA.

phase by the wavelength. Detailed derivations may be found in the literature.<sup>8-10</sup>

Because the DOWR does not remove the ionosphere effect, dual frequency bands are required to remove the ionosphere effect such as the GPS  $L_1$  and  $L_2$  bands.<sup>11</sup> When we define the biased range for frequency bands 1 and 2 as  $R_1$  and  $R_2$ , respectively, the ionosphere free range<sup>9</sup> can be obtained by

$$R = \frac{f_{C1}^2 R_1 - f_{C2}^2 R_2}{f_{C1}^2 - f_{C2}^2} \quad (3)$$

where the effective frequencies can be approximated by

$$f_{Ci} = \sqrt{f_{Ai} f_{Bi}} \quad (4)$$

Satellite A's  $i$ th band frequency is  $f_{Ai}$  and satellite B's is  $f_{Bi}$ . Use of the effective frequency is necessary because two satellites' frequencies for the same frequency band should be slightly different. The frequency offset,  $\Delta f_i$ , is employed to avoid signal interference and to meet other phase-locked loop requirements.<sup>9</sup>

### Effect of Measurement Time-Synchronization Error

One of the error sources of the DOWR system is the measurement time-tag error  $\Delta t_A$  and  $\Delta t_B$ . The intersatellite range error due to the time-tag errors can be approximated as

$$\Delta R_i^t \approx c \frac{f_{Ai} - f_{Bi}}{f_{Ai} + f_{Bi}} (\Delta t_A - \Delta t_B), \quad i = 1, 2 \quad (5)$$

where  $c$  is the speed of light. This equation is for a single-frequency band and has been verified with numerical simulations and ground-test results.<sup>8,10</sup> The range error depends on the relative time-tag error rather than individual absolute error, and the error level is proportional to the carrier frequency offset,  $f_{Ai} - f_{Bi}$ . Therefore, whereas it is desired to minimize the frequency offset, the design limitation noted earlier prevents this.

The range error due to the time-tag error is added to the true range so that the error equation passes through the same ionosphere free combination of Eq. (3). By substituting Eq. (5) into Eq. (3) for the two frequency bands, one can obtain the net range error, due to the time-tag error, after the ionosphere free combination:

$$\Delta R^t = \frac{f_{C1}^2 \Delta R_1^t - f_{C2}^2 \Delta R_2^t}{f_{C1}^2 - f_{C2}^2} \quad (6)$$

### Optimal Solution for Reducing Time-Tag Error Effect

The DOWR system requires the use of dual-frequency bands to achieve a certain level of precision because the ionosphere effect is significant. The necessary use of the dual-frequency bands provides a possibility; cancellation of the time-tag error effect from the two frequency bands.

Because Eq. (6) is the difference between the range errors from the two frequency bands, it may be possible to cancel out the range errors by selecting the frequencies in a certain way, that is, such that the numerator of Eq. (6) becomes zero. With a proper selection of the four frequencies (satellite A's 1 and 2 and satellite B's 1 and 2), the net range error due to the time-tag error can be minimized. Although there are potentially numerous ways to select the optimal frequency ratio, finding the optimal ratio between the two frequency offsets is chosen in this research.

When we define the frequency offsets for frequency bands 1 and 2 as  $\Delta f_1$  and  $\Delta f_2$ , respectively, the ratio of the two offsets can be defined as

$$\alpha = \Delta f_2 / \Delta f_1 \quad (7)$$

The ratio of satellite A's two frequencies can be defined as

$$\beta = f_{A2} / f_{A1} \quad (8)$$

With the ratios of  $\alpha$  and  $\beta$ , satellite A and B's frequencies can be expressed as follows.

Satellite A:

$$f_{A1} = f_{A1}, \quad f_{A2} = \beta f_{A1} \quad (9)$$

Satellite B:

$$f_{B1} = f_{A1} + \Delta f_1, \quad f_{B2} = f_{A2} + \alpha \Delta f_1 = \beta f_{A1} + \alpha \Delta f_1 \quad (10)$$

All four frequencies are expressed in the function of  $f_{A1}$ ,  $\Delta f_1$ ,  $\alpha$ , and  $\beta$ . The goal is to find the optimal ratio of  $\alpha$  to make the net range error of Eq. (6) become zero.

Substituting the four frequencies of Eqs. (9) and (10) into Eq. (5) yields the range error equations for the single-frequency bands  $\Delta R_1^t$  and  $\Delta R_2^t$ . The dual-frequency range error can be obtained by substituting these two range errors into Eq. (6):

$$\Delta R^t = \left\{ c \Delta f_1 \left( \frac{f_{A1}}{2f_{A1} + \Delta f_1} + \frac{\alpha \beta (f_{A1} \beta + \alpha \Delta f_1)}{2f_{A1} \beta + \alpha \Delta f_1} - 1 \right) \right. \\ \left. [f_{A1} + \Delta f_1 - \beta (f_{A1} \beta + \alpha \Delta f_1)] \right\} (\Delta t_A - \Delta t_B) \quad (11)$$

The optimal ratio  $\alpha$  to make the range error zero can be obtained by setting Eq. (11) to zero:

$$\alpha = \frac{\lambda \pm \sqrt{8f_{A1} \beta^2 \Delta f_1 (f_{A1} + \Delta f_1) (2f_{A1} + \Delta f_1) + \lambda^2}}{2\beta \Delta f_1 (2f_{A1} + \Delta f_1)} \quad (12)$$

where

$$\lambda = -2f_{A1} \beta^2 + \Delta f_1^2 + f_{A1} (\Delta f_1 - \beta^2 \Delta f_1) \quad (13)$$

Between the two signs in the numerator, the plus sign yields a feasible solution. In summary, when three frequencies,  $f_{A1}$ ,  $f_{A2}$ , and  $f_{B1}$ , are given with the values of  $f_{A1}$ ,  $\Delta f_1$ , and  $\beta$ , the fourth or satellite B's second band frequency  $f_{B2}$  can be optimally determined with the computed  $\alpha$  value.

### Numerical Simulations

Numerical simulations were performed to validate the optimal solution. Simulated phase measurements were generated from truth intersatellite range and error sources, and the intersatellite range was then estimated and compared with the truth range, where the difference represents the range error level. Detailed simulation procedures have been described elsewhere.<sup>8</sup> The actual GRACE DOWR frequency configuration was selected for a reference and compared with an optimal configuration. Table 1 shows a comparison of the two simulation configurations, 1) GRACE and 2) optimal.

Case 1 refers to the current GRACE KBR configuration.<sup>6,7</sup> The ratio between the two frequency offsets is 1.3333, like the ratio of the K and Ka frequencies. This coincidence is because the two satellites have the same microwave system except for the oscillators. In other words, the frequency offset between the two satellites is realized by the use of slightly different oscillators. The two satellites' oscillator frequencies are changing during the mission lifetime due to the oscillator instability. To prevent possible frequency crossover during the mission, the offset of the K band is set to 0.5 MHz as a minimum

**Table 1** Frequency configurations for simulations

Category	Case 1 (GRACE)	Case 2 (optimal)
Frequency		
$f_{A1}$ , GHz	24.527232	24.527232
$f_{A2}$ , GHz	32.702976	32.702976
$f_{B1}$ , GHz	24.527735	24.528132
$f_{B2}$ , GHz	32.703646	32.703651
Frequency offset		
$\Delta f_1 = f_{B1} - f_{A1}$ , MHz	0.502524	0.900000
$\Delta f_2 = f_{B2} - f_{A2}$ , MHz	0.670032	0.675005
Frequency ratio		
$\alpha$	1.333333	0.750006
$\beta$	1.333333	1.333333

offset.<sup>9</sup> The offset of the Ka band follows the ratio of 1.3333 and becomes 0.67 MHz.

Case 2 refers to an idealized system with an optimal frequency ratio. Satellite A's frequencies are the same as the GRACE configuration, but satellite B's frequencies are modified to have optimal values. To prevent frequency crossover, both K and Ka offsets should be larger than the minimum offset (0.5 MHz). Therefore, the frequency offset of the K band ( $\Delta f_1$ ) is chosen as 0.9 MHz, and this determines satellite B's K-band frequency  $f_{B1}$ . With these three frequencies, the optimal ratio  $\alpha$  is obtained as 0.75006 by using Eq. (12). Then, the offset of the Ka band ( $\Delta f_2$ ) becomes 0.675 MHz, and this value determines satellite B's Ka-band frequency  $f_{B2}$ . Unlike the GRACE configuration, the frequency offset of Ka is smaller than that of K.

Two sets of simulations were performed. One set was an all-error case, which included most significant error sources for the GRACE DOWR; system noise, multipath error, attitude determination error, amplitude modulation/phase modulation noise, etc.<sup>8,10</sup> The only exclusion is the structure variation due to thermal distortion, about 10- $\mu\text{m}$  level because it is not fully modeled yet. The other set was a time-tag-error only case, which isolated the effect of the time-tag error from the other error sources. With different seed numbers for random noise generation, 1000 cases were performed for each case. The time span was 8000 s, and the phase generation interval was 10 s. Each satellite used an independent simulated time-tag error, which represents real-time clock accuracy with an in-flight GPS receiver. Both of the time-tag errors have the same level of standard deviation of 10 ns, but a different bias level of 50 and 10 ns.

Figure 1 shows the range error time series when all of the error sources are applied. The standard deviation values are obtained from 1000 simulation results and the plotted time-series is obtained from one of those results. Each time series is adjusted to have a zero mean by subtracting its mean value (bias). Because the DOWR measurement quantity is inherently the biased range, the bias level

does not need to be addressed. The standard deviation of the error is 43.55  $\mu\text{m}$  with the GRACE configuration (case 1), but the error level is significantly decreased to 2.46  $\mu\text{m}$  with the optimal configuration (case 2). Most of the time-tag error effect is removed with the optimal configuration, and the remaining range error is due to the other error sources. Another set of simulations with a longer time span (86,400 s) was also performed, and they yielded a similar error level.

Figure 2 shows a comparison of the range error time series when only the time-tag error is applied. As in the all-error case, significant reduction of the range error is achieved with the optimal configuration, from 43.41 to 0.07  $\mu\text{m}$ . Comparing the two cases of Figs. 1 and 2, one can conclude that the effect of the inaccurate time tag is significant and may be greater than all other error effects. The use of optimal frequencies will be valuable for applications where the clock offsets are less well known.

## Conclusions

An optimal frequency configuration of high-accuracy intersatellite ranging instruments for real-time use is introduced. The optimal configuration minimizes the range error caused by measurement time-synchronization error, which is critical for DOWR instruments. The numerical simulations demonstrate the advantage of the optimal frequency set over the nonoptimal frequency set, the current GRACE frequency set. Implementation of the optimal frequency may increase the manufacturing cost, for example, manufacturing different sets of multipliers and phase-locked loops for two satellites. However, this approach may benefit future formation-flying missions that require real-time or near real-time high-accuracy intersatellite ranging measurements.

## Acknowledgments

The authors thank Charles Dunn at the Jet Propulsion Laboratory for his comments on this research. The authors are pleased to acknowledge the significant contributions of the Gravity Recovery and Climate Experiment team members around the world.

## References

- MacArthur, J. L., and Posner, A. S., "Satellite-to-Satellite Range-Rate Measurement," *IEEE Transactions on Geoscience and Remote Sensing*, Vol. GE-23, No. 4, 1985, pp. 517–523.
- Pisacane, V. L., Ray, J. C., MacArthur, J. L., and Bergeson-Willis, S. E., "Description of the Dedicated Gravitational Satellite Mission (GRAVSAT)," *IEEE Transactions on Geoscience and Remote Sensing*, Vol. GE-20, No. 3, 1982, pp. 315–321.
- Yionoulis, S. M., and Pisacane, V. L., "Geopotential Research Mission: Status Report," *IEEE Transactions on Geoscience and Remote Sensing*, Vol. GE-23, No. 4, 1985, pp. 511–516.
- Davis, E. S., Dunn, C. E., Stanton, R. H., and Thomas, J. B., "The GRACE Mission: Meeting the Technical Challenges," International Astronautical Federation, Paper IAF-99-B.2.05, Oct. 1999.
- Kim, J., and Tapley, B. D., "Error Analysis of a Low-Low Satellite-to-Satellite Tracking Mission," *Journal of Guidance, Control, and Dynamics*, Vol. 25, No. 6, 2002, pp. 1100–1106.
- Dunn, C., Bertiger, W., Bar-Sever, Y., Desai, S., Haines, B., Kuang, D., Franklin, G., Harris, I., Kruizinga, G., Meehan, T., Nandi, S., Nguyen, D., Rogstad, T., Thomas, B., Tien, T. J., Romans, L., Watkins, M., Wu, S.-C., Bettadpur, S., and Kim, J., "Application Challenge: Instrument of Grace GPS Augments Gravity," *GPS World*, Vol. 14, No. 2, 2003, pp. 16–28.
- Bertiger, W., Bar-Sever, Y., Desai, S., Dunn, C., Haines, B., Kruizinga, G., Kuang, D., Nandi, S., Romans, L., Watkins, M., and Wu, S., "GRACE: Millimeters and Microns in Orbit," *Proceedings of ION GPS 2002*, Inst. of Navigation, 2002, pp. 2022–2029.
- Kim, J., and Tapley, B. D., "Simulation of Dual One-Way Ranging Measurements," *Journal of Spacecraft and Rockets*, Vol. 40, No. 3, 2003, pp. 419–425.
- Thomas, J. B., "An Analysis of Gravity-Field Estimation Based on Intersatellite Dual-1-Way Biased Ranging," Jet Propulsion Lab., JPL Publ. 98-15, Pasadena, CA, May 1999.
- Kim, J., "Simulation Study of a Low-Low Satellite-to-Satellite Tracking Mission," Ph.D. Dissertation, Dept. of Aerospace Engineering and Engineering Mechanics, Univ. of Texas, Austin, TX, May 2000.
- Leick, A., *GPS Satellite Surveying*, 2nd ed., Wiley, New York, 1995, pp. 247–271.

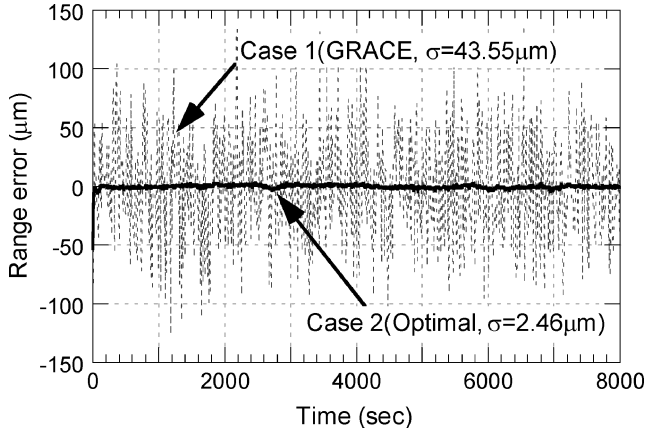


Fig. 1 Range error time series with all error sources.

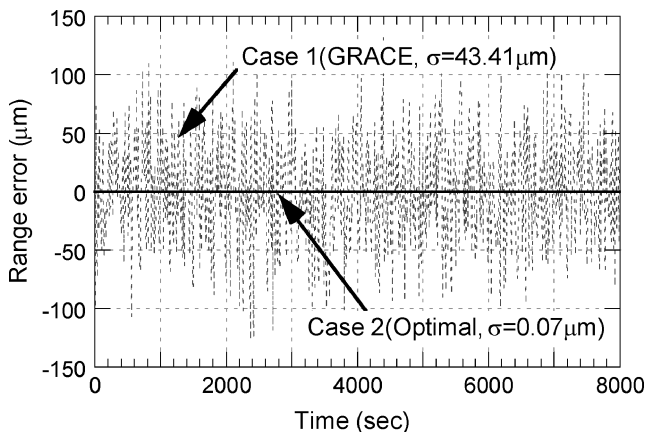


Fig. 2 Range error time series with time-tag error only.